Deposition of High-Quality HfO_2 on Graphene and the Effect of Remote Oxide Phonon Scattering

K. Zou,[1] X. Hong,[1] D. Keefer,[2,3] and J. Zhu[1]

[1]*Department of Physics, The Pennsylvania State University, University Park, Pennsylvania 16802, USA*
[2]*Department of Chemistry, Beloit College, Beloit, Wisconsin 53511, USA*
[3]*Department of Chemistry, The Pennsylvania State University, University Park, Pennsylvania 16802, USA*

(Received 28 January 2010; published 16 September 2010)

We demonstrate atomic layer deposition of high-quality dielectric HfO_2 films on graphene and determine the magnitude of remote oxide surface phonon scattering in dual-oxide structures. The carrier mobility in these HfO_2-covered graphene samples reaches 20 000 $cm^2/V\,s$ at low temperature. Distinct contributions to the resistivity from surface optical phonons in the SiO_2 substrate and the HfO_2 overlayer are isolated. At 300 K, surface phonon modes of the HfO_2 film centered at 54 meV limit the mobility to approximately 20 000 $cm^2/V\,s$.

DOI: 10.1103/PhysRevLett.105.126601 PACS numbers: 72.80.Vp, 71.38.−k, 73.43.Qt, 73.50.Dn

Charge traps and remote optical phonons in adjacent dielectric oxide layers reduce the electron mobility μ of silicon inversion layers [1–4]. Similar phenomena occur in graphene field effect transistors (GFETs) supported on a substrate [5–7]. Understanding and controlling how the oxide affects electron transport is critical to achieving the promise of intrinsic graphene. Local top gating of graphene, which requires a top-gate dielectric, is essential to constructing advanced electronic device structures for both fundamental studies and practical applications [8–13]. Several materials have been used as gate oxides in GFETs [8–14], but little is known quantitatively about their effects on electron transport. Furthermore, the effect of oxides on transport in *double-oxide* structures has not been studied. Such structures are essential to advancing the study of the graphene two-dimensional electron gas.

In this Letter, we reveal the effects of remote oxide phonon (ROP) scattering on the electron mobility in double-oxide HfO_2/graphene/SiO_2 structures, quantitatively extracting distinct contributions from both oxides. The high quality of the HfO_2 deposition enables a low-temperature field effect mobility μ_{FE} as high as $\sim$20 000 $cm^2/V\,s$ in HfO_2-covered graphene, the highest reported so far for graphene covered by atomic layer deposition-grown oxides and comparable to that of the best pristine exfoliated graphene on substrates [15,16]. At elevated temperatures, μ decreases rapidly due to ROP scattering from the SiO_2 substrate and the HfO_2 overlayer, with the low-energy modes of the HfO_2 overlayer dominating. This mechanism limits μ to 20 000 $cm^2/V\,s$ at 300 K.

We first fabricate conventional GFETs on SiO_2 by using mechanically exfoliated graphene [14]. HfO_2 films are then patterned and deposited on graphene by using atomic layer deposition at 110 °C using two precursors: H_2O and $Hf(NMe_2)_4$ [17]. Figure 1 shows an optical micrograph of a GFET partially covered by 30 nm of HfO_2 and an atomic force microscope image of the area between two metal contacts. In all devices, the HfO_2 film appears amorphous and smooth, growing continuously across the graphene/SiO_2 step with a step height typical of single-layer graphene [7 Å in Fig. 1(b)]. These observations provide initial evidence of a high-quality gate oxide. We find that HfO_2 can also grow on pristine exfoliated single-layer graphene directly without a seeding layer. Films thicker than 10 nm are typically pinhole-free and show excellent morphology, with rms roughness of 2–3 Å (Fig. S1 in Ref. [17]). In contrast, films grown on multilayer (5–6 layers) graphene sheets show much poorer coverage (Fig. S2 in Ref. [17]), consistent with previous studies [18–20]. This observation leads us to speculate that curvature induced by the underlying SiO_2 substrate in single-layer graphene facilitates the adsorption and reaction of the precursors. Details of the growth on pristine single and multilayer graphene, as well as the assessment of a poly(methyl methacrylate) interfacial layer on graphene devices, are given in the supporting information [17].

We determine the static dielectric constant of the HfO_2 film through its gating efficiency on graphene, obtaining

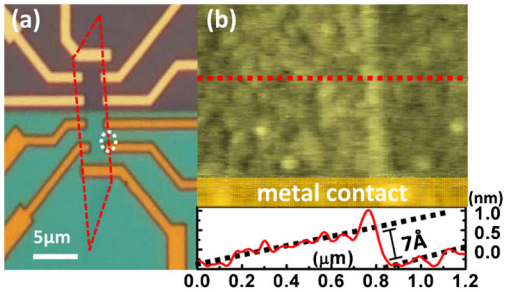

FIG. 1 (color online). (a) Optical micrograph of a GFET partially covered by 30 nm HfO_2 film (bottom half, green). The graphene sheet is outlined in red. (b) Atomic force microscope image of the circled area in (a) and a line cut across the graphene/SiO_2 step. The rms roughness is 3–4 Å on graphene and 2–3 Å on SiO_2.

$\epsilon^0 = 17 \pm 0.2$, in agreement with values reported in previous low-temperature (90–150 °C) growth [9,21]. Top gates using 30 nm HfO_2 as the dielectric layer have a gate efficiency of $\sim 3.1 \times 10^{12}$ cm^2/V and can induce more than 1.5×10^{13}/cm^2 carriers into graphene, exceeding the range of the SiO_2 back gate ($\sim 1 \times 10^{13}$/cm^2 at 140 V). The high dielectric constant and excellent breakdown characteristics of HfO_2 enable large, efficient charge accumulation in graphene transistors.

Resistivity and quantum Hall measurements are performed in a He^4 cryostat with a 9 T magnet by using standard low-frequency lock-in techniques with currents of 50–100 nA. We report results on three partially covered GFET samples: *A*, *B*, and *C*. Figure 2(a) plots the 4-terminal low-T sheet conductance $\sigma(V_{bg})$ on the HfO_2 side of these samples. The low-density field effect mobilities $\mu_{FE} = (d\sigma/dn)(1/e)$ are 9600, 17 000, and 11 200 cm^2/V s [22]. These values are close to μ_{FE} on the bare side of the same device: 11 500, 16 100, and 10 400 cm^2/V s, respectively [23–25]. These mobilities exceed the best $\mu_{FE} = 8600$ cm^2/V s reported for graphene covered by atomic layer deposition-grown oxides [11,15,16] and are comparable to the best pristine exfoliated samples. In addition to high μ, HfO_2-covered samples exhibit well-developed half-integer quantum Hall states [Fig. 2(b)] and magnetoresistance oscillations [Fig. S4(b) in Ref. [17]] similar in quality to those of pristine exfoliated graphene [26]. These observations attest to the highly homogenous electron density of our samples. Raman spectra obtained on both the bare and the HfO_2 side of the GFETs are comparable to pristine graphene, with no visible *D* peak [17].

At elevated temperatures, electrons in graphene are subject to scattering by polar optical phonon modes in nearby oxide layers [1]. This mechanism is an important mobility-limiting factor in silicon transistors, especially those using high-κ oxides with low-energy phonon modes [3]. We measure the T-dependent resistivity $\rho(T)$ in samples *A*, *B*, and *C* on both bare and HfO_2-covered sides from 10 to 250 K [27] for carrier densities $1 \times 10^{12}/\text{cm}^2 < n < 3 \times 10^{12}/\text{cm}^2$. Figure 3 gives the results from sample *B*, plotting $\rho(T)$ on the bare and covered side separately in (a) and (b) at several densities and together for comparison in (c) at $n = 3 \times 10^{12}/\text{cm}^2$. From 10 to 100 K, $\rho(T)$ increases linearly with T with the same slope, 0.1 Ω/K, on both the bare and HfO_2-covered sides. Previously, this linear-T dependence was attributed to longitudinal acoustic (LA) phonon scattering [5,28]: $\rho_{LA}(T) = (h/e^2)\pi^2 D_A^2 k_B T/(2h^2 \rho_s v_s^2 v_F^2)$. Our data support this conclusion. Fitting to Eq. (1) yields a deformation potential $D_A = 18 \pm 2$ eV across all samples, in good agreement with $D_A = 18 \pm 1$ eV obtained by Chen *et al.* [5].

Above 100 K, $\rho(T)$ increases supralinearly with T on both sides of the GFET, with a steeper dependence on the HfO_2-covered side in all samples. This rapid rise in $\rho(T)$ was observed in graphene on SiO_2 and attributed to either remote substrate phonon scattering [5,7] or the thermal activation of quenched ripples [6]. Our results show that the deposition of a HfO_2 overlayer consistently increases the resistance. This observation is difficult to reconcile with a quenched ripple scenario; instead, it strongly suggests the existence of a new scattering channel. We incorporate the possible contribution from remote optical phonons in the HfO_2 layer as follows:

$$\rho(T, n) = \rho_0(n) + \rho_{LA}(T) + \rho_{ROP}(T, n), \qquad (1)$$

where $\rho_0(n)$ represents the low-T residual resistivity, $\rho_{LA}(T)$ is the LA phonon contribution described earlier,

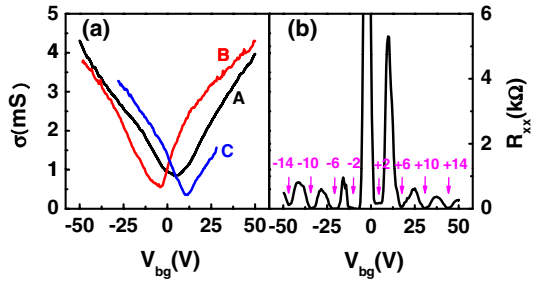

FIG. 2 (color online). (a) Low-T sheet conductance $\sigma(V_{bg})$ of the HfO_2-covered side in three partially covered GFETs (samples *A*, *B*, and *C* are black, red, and blue, respectively). The majority of our HfO_2-covered samples exhibit Dirac points within ±20 V and $\mu_{FE} > 6000$ cm^2/V s. (b) Well-developed half-integer quantum Hall states on the HfO_2-covered side of sample *A* at $B = 8.9$ T and $T = 1.5$ K.

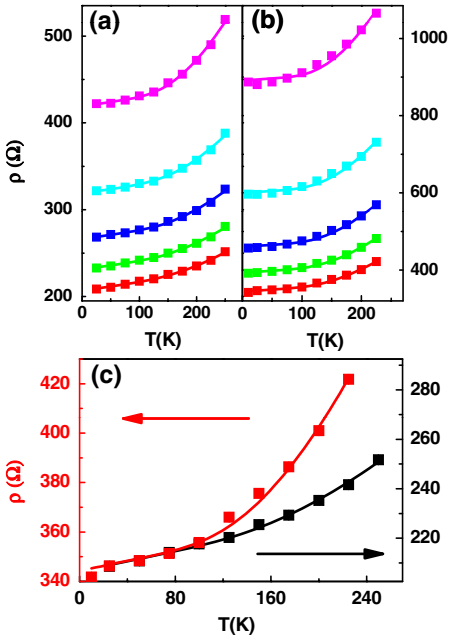

FIG. 3 (color online). Resistivity $\rho(T)$ on the bare (a) and HfO_2-covered (b) sides of sample *B*. From top to bottom: Hole density $n = 1.0$–$3.0 \times 10^{12}/\text{cm}^2$ in $5.0 \times 10^{11}/\text{cm}^2$ steps. Error bars are smaller than the symbol size. (c) $\rho(T)$ at $n = 3.0 \times 10^{12}/\text{cm}^2$ for the bare (black) and covered sides (red). Solid lines are fits to Eq. (1).

and $\rho_{\mathrm{ROP}}(T, n)$ originates from remote oxide phonon scattering. $\rho_{\mathrm{ROP}}(T, n)$ is given by

$$\rho_{\mathrm{ROP}}(T, n) = \int A(\mathbf{k}, \mathbf{q}) d\mathbf{k} d\mathbf{q} \sum_i g_i / (e^{\hbar\omega_i/k_B T} - 1), \quad (2)$$

where $A(\mathbf{k}, \mathbf{q})$ is the matrix element for scattering between electron ($\mathbf{k}$) and phonon ($\mathbf{q}$) states and ω_i and g_i represent the frequency and coupling strength, respectively, of the ith surface optical phonon mode [1,3,7]. Both ω_i and g_i can be calculated by using the frequencies of the transverse and longitudinal optical phonon modes in the bulk oxide and the static, intermediate, and optical dielectric constants of the material [3]. On the vacuum/graphene/SiO_2 side of the GFET, two ROP modes from the SiO_2 substrate are important [5,7]. Following the approach of Ref. [3] and using dielectric constants measured for our substrates, we obtain $\omega_1 = 63$ meV, $\omega_2 = 149$ meV, $g_1 = 3.2$ meV, and $g_2 = 8.7$ meV. Details of the calculation are given in the supporting information [17].

We define a density-dependent resistivity coefficient $C_i(n) = g_i \int A(\mathbf{k}, \mathbf{q}) d\mathbf{k} d\mathbf{q}$ and rewrite Eq. (2) as follows:

$$\rho_{\mathrm{ROP}}(T, n) = \sum_i C_i(n) / (e^{\hbar\omega_i/k_B T} - 1). \quad (3)$$

Equations (1)–(3) provide an excellent description of $\rho(T, n)$ on the bare side of the GFET, as shown in Fig. 3(a). Contributions from the ω_2 mode are negligible in the temperature range studied, as expected from Eq. (2) and verified by the fits. The $C_1(n)$ of the ω_1 mode is plotted in Fig. 4(a) for all samples. $C_1(n)$ follows an approximate $1/n$ density dependence and varies less than 25% among our samples, including conventional graphene-on-SiO_2 devices not shown here. They are also in excellent agreement with values reported by Chen *et al.* [5]. The consistency and reproducibility of $\rho(T)$ further supports the remote optical phonon model, since scattering from quenched ripples is likely to vary from sample to sample.

We determine the frequency and coupling strength of the ROP mode in the HfO_2 film by directly measuring its infrared absorption spectra and static and optical dielectric constants [17]. In contrast to crystalline HfO_2, which exhibits well-defined transverse and longitudinal optical phonon modes in the range 100–700 cm^{-1} [3], our *amorphous* HfO_2 films show a broad absorption maximum centered at 320 cm^{-1} [17,29]. Approximating the corresponding distribution of surface phonon modes with a single frequency ω_3, we obtain $\omega_3 = 54$ meV. Because of the new dielectric geometry $\epsilon_{\mathrm{SiO_2}}(\omega) + \epsilon_{\mathrm{HfO_2}}(\omega) = 0$, the HfO_2 overlayer also modifies the frequency of the existing SiO_2 surface modes slightly and screens the coupling strength of the above modes. On the HfO_2-covered side, we obtain $\omega_1' = 72$ meV, $g_1' = 1.2$ meV (SiO_2), $\omega_2' = 143$ meV, $g_2' = 2.4$ meV (SiO_2), and $\omega_3 = 54$ meV, $g_3 = 5.7$ meV (HfO_2). Details of the calculation are given in the supporting information [17].

$\rho(T, n)$ on the HfO_2 side of samples A, B, and C are fit to Eqs. (1) and (3) considering two surface phonon modes ω_1' and ω_3. The two frequencies are too close to be differentiated by the fitting itself. Instead, $C_1'(n) = C_1(n)/2.6$ is used as input to Eq. (1) to extract $C_3(n)$. The fits describe the data very well, as shown in Fig. 3(b). Figure 4(b) plots the resulting $C_3(n)$. Despite the approximation used to describe the HfO_2 phonons, the experimentally determined ratio $C_3(n)/C_1'(n)$, which ranges from 2.5 to 5.5, agrees well with the predicted ratio $g_3/g_1' = 4.7$. The n dependence of $C_1(n)$ and $C_3(n)$ and the variation of $C_3(n)$ among samples are discussed in the supporting information in the context of electron screening and the effect of a spacing layer at the graphene-oxide interface [17]. Overall, this analysis demonstrates the success of the ROP scattering model in explaining the magnitude and T dependence of $\rho(T, n)$ in HfO_2/graphene/SiO_2 structures.

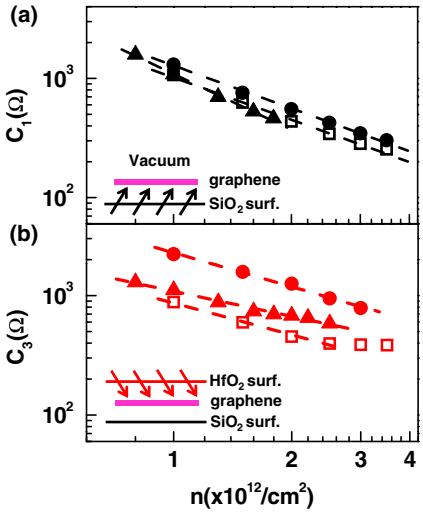

FIG. 4 (color online). (a) Resistivity coefficient vs density $C_1(n)$ of the $\omega_1 = 63$ meV mode of the SiO_2 surface on the bare side of three GFETs. (b) $C_3(n)$ of the $\omega_3 = 54$ meV mode of the HfO_2 surface on the covered side of the same GFETs. Open squares, solid circles, and solid triangles correspond to samples A–C, respectively. Dashed lines are empirical fittings to $n^{-\alpha}$, where α range from 1.1 to 1.6 for $C_1(n)$ and from 0.7 to 1.0 for $C_3(n)$. Electrons and holes exhibit similar $C(n)$.

Figure 5 summarizes the magnitude of the various phonon scattering mechanisms by plotting $\mu_i(n) = 1/ne\rho_i(n)$ determined for each phonon channel in sample B. At 300 K, the LA phonon of graphene produces $\mu \sim 1/n$, which is approximately $1 \times 10^5\ \mathrm{cm}^2/\mathrm{V\,s}$ at $n = 2 \times 10^{12}/\mathrm{cm}^2$. Surprisingly, the ROP modes of the SiO_2 substrate, while limiting μ to $\sim$60 000 $\mathrm{cm}^2/\mathrm{V\,s}$ in single-oxide devices, play a minor role in HfO_2/graphene/SiO_2 devices due to screening from the HfO_2 overlayer, producing only $\mu \sim 2 \times 10^5\ \mathrm{cm}^2/\mathrm{V\,s}$. At 300 K, the ROP mode of the HfO_2 overlayer dominates the scattering and limits μ to approximately 20 000 $\mathrm{cm}^2/\mathrm{V\,s}$. These results provide key insight into the design of graphene electronics. While high-κ oxides such as HfO_2 enable efficient carrier injection, their negative effect on carrier mobility must be taken into account.

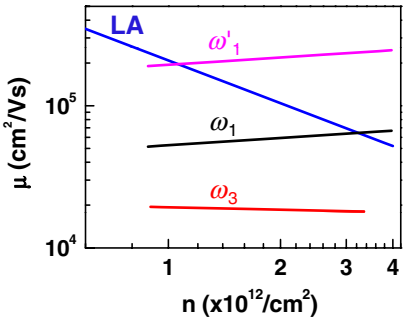

FIG. 5 (color online). Mobility limit imposed by LA and ROP scattering at 300 K in sample B. $\omega_1 = 63$ meV is the dominant surface mode in graphene-on-SiO_2 samples (black). ω'_1 represents the corresponding screened mode in HfO_2/graphene/SiO_2 structures (magenta). The $\omega_3 = 54$ meV mode in HfO_2 covered GFETs limits μ to 20 000 $cm^2/V\,s$ (red). The blue line represents μ set by LA phonons.

In conclusion, we demonstrate atomic layer deposition of high-quality HfO_2 film on graphene and report one of the highest mobility among oxide-covered GFETs, $\mu \sim$ 10 000–20 000 $cm^2/V\,s$. Remote surface phonons in the HfO_2 film scatter strongly at high temperature and hence limit carrier mobility in graphene to 20 000 $cm^2/V\,s$ at 300 K. Our results provide valuable insight to understand the behavior of two-dimensional electron gases in graphene and guide the design and performance optimization of graphene transistors. The methods employed here may be generalized to characterize other substrates and top-gate oxides in single-gated and double-gated FETs.

We are grateful for helpful discussions with Vin Crespi, Peter Eklund, Simone Fratini, Jainendra Jain, and Jerry Mahan. Xiaoming Liu assisted with infrared absorption spectra. This work is supported by NSF CAREER DMR-0748604 and NSF NIRT ECS-0609243. D. K. acknowledges the NSF NNIN REU-0335765. The authors acknowledge the PSU site of NSF NNIN.

Note added.—More recently, several studies demonstrate the essential role played by remote oxide phonons in the energy dissipation and current saturation process in graphene transistors operating at large source-drain bias [30–32].

[1] S. Wang and G. Mahan, Phys. Rev. B **6**, 4517 (1972).
[2] T. Ando, A. Fowler, and F. Stern, Rev. Mod. Phys. **54**, 437 (1982).
[3] M. Fischetti, D. Neumayer, and E. Cartier, J. Appl. Phys. **90**, 4587 (2001).
[4] J. Robertson, Rep. Prog. Phys. **69**, 327 (2006).
[5] J. Chen, C. Jang, S. Xiao, M. Ishigami, and M. Fuhrer, Nature Nanotech. **3**, 206 (2008).
[6] S. Morozov, K. Novoselov, M. Katsnelson, F. Schedin, D. Elias, J. Jaszczak, and A. Geim, Phys. Rev. Lett. **100**, 016602 (2008).
[7] S. Fratini and F. Guinea, Phys. Rev. B **77**, 195415 (2008).
[8] J. Williams, L. Dicarlo, and C. Marcus, Science **317**, 638 (2007).
[9] I. Meric, M. Han, A. Young, B. Ozyilmaz, P. Kim, and K. Shepard, Nature Nanotech. **3**, 654 (2008).
[10] J. B. Oostinga, H. B. Heersche, X. Liu, A. F. Morpurgo, and L. M. K. Vandersypen, Nature Mater. **7**, 151 (2008).
[11] S. Kim, J. Nah, I. Jo, D. Shahrjerdi, L. Colombo, Z. Yao, E. Tutuc, and S. Banerjee, Appl. Phys. Lett. **94**, 062107 (2009).
[12] N. Stander, B. Huard, and D. Goldhaber-Gordon, Phys. Rev. Lett. **102**, 026807 (2009).
[13] D. Farmer, Y. Lin, A. Afzali-Ardakani, and P. Avouris, Appl. Phys. Lett. **94**, 213106 (2009).
[14] X. Hong, A. Posadas, K. Zou, C. Ahn, and J. Zhu, Phys. Rev. Lett. **102**, 136808 (2009).
[15] After the submission of the manuscript, we become aware of Ref. [16], which reports μ_{FE} up to 23 600 $cm^2/V\,s$ by using oxide nanoribbons mechanically transferred onto graphene as the top-gate dielectric.
[16] L. Liao, J. Bai, Y. Qu, Y.-c. Lin, Y. Li, Y. Huang, and X. Duan, Proc. Natl. Acad. Sci. U.S.A. **107**, 6711 (2010).
[17] See supplementary material at http://link.aps.org/supplemental/10.1103/PhysRevLett.105.126601 for device fabrication, HfO_2 growth, Raman, additional transport data, calculations of phonons, and discussions.
[18] X. Wang, S. Tabakman, and H. Dai, J. Am. Chem. Soc. **130**, 8152 (2008).
[19] B. Lee, S. Park, H. Kim, K. Cho, E. Vogel, M. Kim, R. Wallace, and J. Kim, Appl. Phys. Lett. **92**, 203102 (2008).
[20] Y. Xuan, Y. Wu, T. Shen, M. Qi, M. Capano, J. Cooper, and P. Ye, Appl. Phys. Lett. **92**, 013101 (2008).
[21] M. Biercuk, D. Monsma, C. Marcus, J. Becker, and R. Gordon, Appl. Phys. Lett. **83**, 2405 (2003).
[22] The electron-hole asymmetry in $\sigma(V_{bg})$ is presumably due to contacts. The higher μ_{FE} of the two carrier types is reported here.
[23] A possible spacing layer at the HfO_2/graphene interface prevents us from examining the dielectric screening effect of the HfO_2 overlayer. See [17] and Refs. [24,25] for details.
[24] C. Jang, S. Adam, J. H. Chen, E. D. Williams, S. Das Sarma, and M. S. Fuhrer, Phys. Rev. Lett. **101**, 146805 (2008).
[25] L. Ponomarenko, R. Yang, T. Mohiuddin, M. Katsnelson, K. Novoselov, S. Morozov, A. Zhukov, F. Schedin, E. Hill, and A. Geim, Phys. Rev. Lett. **102**, 206603 (2009).
[26] X. Hong, K. Zou, and J. Zhu, Phys. Rev. B **80**, 241415 (2009).
[27] $\rho(T)$ data above 250 K are not used here due to hysteresis in back-gate sweeps.
[28] E. Hwang and S. Das Sarma, Phys. Rev. B **77**, 115449 (2008).
[29] D. Ceresoli and D. Vanderbilt, Phys. Rev. B **74**, 125108 (2006).
[30] M. Freitag, M. Steiner, Y. Martin, V. Perebeinos, Z. Chen, J. C. Tsang, and P. Avouris, Nano Lett. **9**, 1883 (2009).
[31] A. M. DaSilva, K. Zou, J. K. Jain, and J. Zhu, Phys. Rev. Lett. **104**, 236601 (2010).
[32] V. Perebeinos and P. Avouris, Phys. Rev. B **81**, 195442 (2010).